Laser plasma acceleration of electrons: Towards the production of monoenergetic beams[a)]

K. Krushelnick,[b)] Z. Najmudin, S. P. D. Mangles, A. G. R. Thomas, M. S. Wei, B. Walton, A. Gopal, E. L. Clark, and A. E. Dangor
Blackett Laboratory, Imperial College, London SW7 2BZ, United Kingdom

S. Fritzler
Laboratoire d'Optique Appliquée, École Nationale Superieure des Techniques Avancées, École Polytechnique, CNRS, UMR 7639, 91761 Palaiseau, France

C. D. Murphy and P. A. Norreys
Central Laser Facility, Rutherford Appleton Laboratory, Chilton, Didcot, Oxon OX11 0QX, United Kingdom

W. B. Mori
Department of Physics, University of California, Los Angeles, California 90095

J. Gallacher, D. Jaroszynski, and R. Viskup
Department of Physics, University of Strathclyde, Glasgow G4 0NG, United Kingdom

(Received 18 November 2004; accepted 2 March 2005; published online 2 May 2005)

The interaction of high intensity laser pulses with underdense plasma is investigated experimentally using a range of laser parameters and energetic electron production mechanisms are compared. It is clear that the physics of these interactions changes significantly depending not only on the interaction intensity but also on the laser pulse length. For high intensity laser interactions in the picosecond pulse duration regime the production of energetic electrons is highly correlated with the production of plasma waves. However as intensities are increased the peak electron acceleration increases beyond that which can be produced from single stage plasma wave acceleration and direct laser acceleration mechanisms must be invoked. If, alternatively, the pulse length is reduced such that it approaches the plasma period of a relativistic electron plasma wave, high power interactions can be shown to enable the generation of quasimonoenergetic beams of relativistic electrons.
 [DOI: 10.1063/1.1902951]

I. INTRODUCTION

The technology of high power lasers has advanced significantly over the past several years. It is now possible to perform experiments with high energy "Petawatt" (10^{15} Watts) class laser systems at large laser facilities and equally possible to perform high intensity experiments using ultrashort pulse laser systems (sub 50 fs) which have high repetition rates and which fit into a university scale laboratory.[1] Both of these types of lasers are capable of producing unique states of matter which can have relativistic "temperatures,"[2] ultrastrong magnetic fields[3] and which can produce beams of energetic electrons,[4,5] ions,[6] and γ rays.[7] This has consequently led to a recent surge of interest in these systems for technological applications as well as for the examination of fundamental scientific issues.

A particularly exciting application of laser produced plasmas is the potential development of high field, "compact" electron accelerators.[4,8] In recent experiments we have evaluated the use of both a Petawatt class laser and a high repetition rate ultrashort pulse system for relativistic electron acceleration applications. The acceleration mechanism for most previous experiments has been the production of relativistic plasma waves, which can trap and accelerate electrons. We have found that for interactions in the "picosecond" pulse-duration regime the electron acceleration mechanism changes from relativistic plasma wave acceleration to direct laser acceleration as the intensity is increased. The limiting electron energy for plasma wave acceleration is due to the well known dephasing limit—however, for direct acceleration mechanisms the ultimate limit is not clear. Although the relativistic electron bunches generated from these experiments are highly directional and contain high charge, they are emitted with an extremely large energy spread which makes many of the potentially important applications for electron beams unfeasible with these sources.

However, in recent experiments also described here, we show that only in high power experiments using much shorter pulses (in the tens of femtoseconds regime) is it possible to generate true "beams" of relativistic electrons which have low divergence and which have a relatively small energy spread ($<5\%$).[9,10]

This is an extremely important result since only if narrow energy bandwidths are achievable will the full range of applications become possible. The use of plasma acceleration consequently now offers the potential of significantly smaller and cheaper facilities for generating energetic electron beams, which, considered along with the current rapid devel-

[a)]Paper FI2 4, Bull. Am. Phys. Soc. **49**, 137 (2004).
[b)]Invited speaker.

opments in laser technology, could soon allow the construction of university laboratory sized accelerators for use in a wide range of experiments and applications. For example, table-top narrow band femtosecond x-ray sources and free-electron lasers could become a reality—which may potentially lead to significant advances in both medicine and material science. It may also be possible to use electron bunches generated in this way for injection into conventional rf accelerators or into subsequent plasma acceleration stages.

II. SELF-MODULATED LASER WAKEFIELD ACCELERATION

High field electron acceleration techniques typically rely on electron plasma waves as the accelerating medium. In the laser wakefield accelerator concept,[8] these waves are excited immediately behind the laser pulse as it propagates through the plasma. Efficient energy transfer between the plasma wave and the electrons requires that both move at similar velocities and this is achieved through the use of low density plasmas (less than 10^{20} cm^{-3}), in which the phase velocity of the laser-excited plasma wave is equal to the laser pulse group velocity (which is close to the speed of light in vacuum). The longitudinal electric fields associated with the relativistic plasma waves are then able to accelerate relativistic particles injected externally, or even, for large amplitude waves, to trap particles from the plasma itself. Subsequently, particles can be boosted to high energy over very short distances by "surfing" on this electrostatic wave.

Acceleration schemes using lasers use the ponderomotive force of either a single very short pulse or a train of very short light pulses, each tailored to resonantly drive the relativistic plasma wave (resonance occurs when the laser pulse duration is about half of the electron plasma period T_p).

Thus far, the schemes studied for producing wakefields are the laser wakefield accelerator (LWFA),[8] the laser beat wave accelerator (LBWA),[11,12] the self-modulated laser wakefield accelerator (SM-LWFA),[5,13] and the forced laser wakefield (F-LWFA) (Ref. 14) accelerator. In the LWFA the laser pulse pushes electrons at its leading and trailing edges with optimal coupling when the resonance condition mentioned above is satisfied. Electrons injected at 3 MeV have been accelerated by this scheme up to 4.7 MeV.[15] In the LBWA, a train of short pulses (a beat frequency) is produced by copropagating two laser pulses at slightly different wavelengths. Electric fields close to the GV/m level have been measured for this experimental configuration using CO_2 laser beams and injected electrons have been accelerated up to 30 MeV.[11] In both LWFA and LBWA, only electrons injected externally into the wave have been accelerated. In contrast, in the SM-LWFA and F-LWFA schemes, the plasma wave amplitude becomes so large that electrons from the plasma itself are trapped by the wave and are boosted to very high energies (i.e., the plasma wave breaks so that no external electron source is needed).

The SM-LWFA regime uses long ($\tau_L \gg T_p$) laser pulses at intensities sufficient to strongly excite the self-modulation instability which is related to stimulated forward Raman scattering. In this process, the laser pulse self-focuses and scatters upon encountering electron plasma waves. The beating of the scattered electromagnetic wave with the laser light amplifies the plasma waves, leading to instability and plasma wave growth. As a result, the initial laser pulse is strongly modulated and is gradually transformed into a train of very short pulses that naturally satisfy the resonance condition. The plasma can also act as a converging lens due to relativistic effects and can focus the laser beam, permitting interactions at higher intensity than in vacuum and over a longer distance than the natural diffraction length.

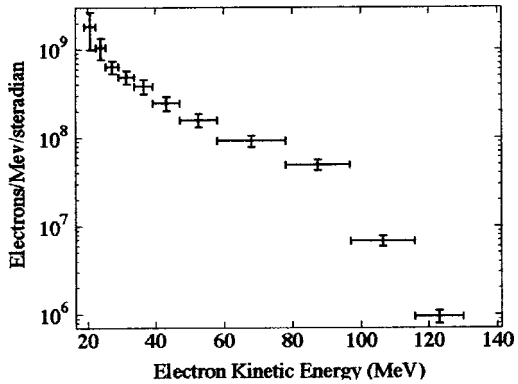

FIG. 1. Typical electron spectrum from self-modulated laser wakefield from a 50 TW laser interaction with a helium gas jet target ($n_e = 3 \times 10^{19}$ cm^{-3}).

An example of an electron spectrum from a SM-LWFA experiment is shown in Fig. 1. This was produced from a laser plasma interaction experiment using the 50 TW VULCAN laser system at the Rutherford Appleton Laboratory. This interaction was performed at a plasma density of $\sim 3 \times 10^{19}$ cm^{-3} and a laser intensity of $\sim 10^{19}$ W cm^{-2} and a pulse length of about 1 ps. In this regime the peak electron energy observed was about 120 MeV—although because the acceleration mechanism is caused by an instability, experiments in this regime are characterized by considerable shot-to-shot fluctuations in the peak electron energy and in the total accelerated charge. Typical forward scattered laser spectra are shown in Fig. 2. These show the characteristic scattered anti-Stokes sidebands (separated by the electron plasma frequency) which can be correlated to the production of the relativistic electron beam. The behavior of the sidebands on the Stokes (downshifted) side of the laser frequency is similar.[16] As the plasma density increases the number of accelerated electrons can also dramatically increase—due to "wave breaking" of the waves and self-trapping of electrons in the wake. This is evident in the forward scattered spectrum as a distinct broadening of the sidebands [see Fig. 2(b)] due to the transition from scattering from a large amplitude "single frequency" plasma wave to a scattering from a nonlinear "broken" wave.

The divergence of the high energy electrons from interactions in the SM-LWFA typically increases with density and can reach values up to 15° for electrons greater than 8 MeV (see Fig. 3 where the electron beam divergence has been measured using activation techniques).

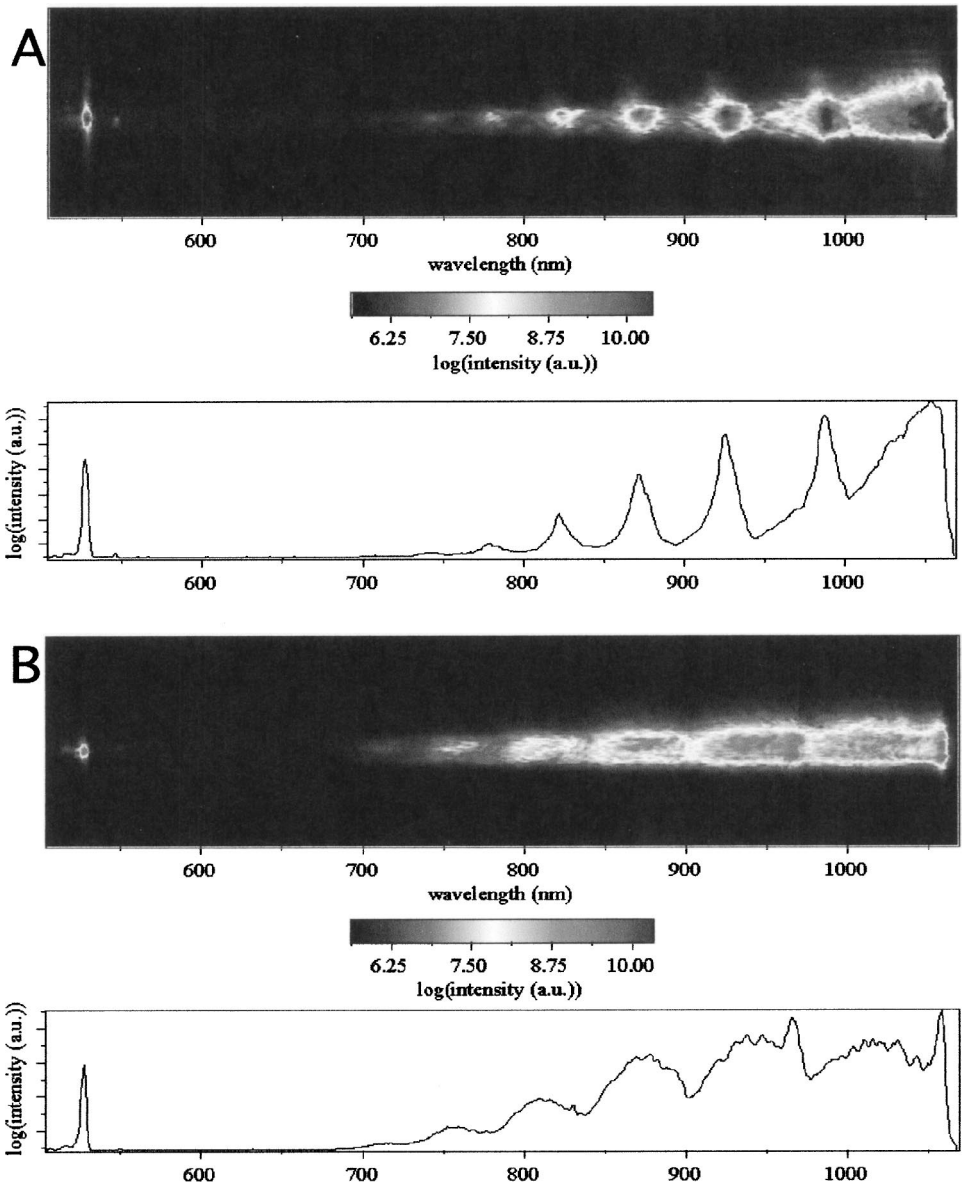

FIG. 2. Transmitted beam spectra with (a) $n_e=4\times10^{18}$ cm^{-3} and $I=2\times10^{19}$ W cm^{-2} and (b) $n_e=7.5\times10^{18}$ cm^{-3} and $I=1\times10^{19}$ W cm^{-2}. The signal at 527 nm is due to the second harmonic. Stokes satellites (down shifted satellites) are not shown because the CCD detector used is not sensitive at those wavelengths.

III. LASER ACCELERATION OF ELECTRONS AT INTENSITIES GREATER THAN 10^{20} W/cm^2

The recent development of Petawatt class lasers such as that at the Central Laser Facility at the Rutherford Appleton Laboratory in the UK has allowed experiments to be performed at much higher intensities than previously available. The intensity of a laser system is often described by the normalized vector potential of the laser field $a_0=eA/mc^2$ (A is the vector potential of the laser field and m is the electron mass). a_0 is also the normalized transverse momentum of the electron motion in the laser field. As a_0 approaches 1 the electron motion becomes relativistic. The previous experiments as described in Sec. II were performed with a_0 between 1 and 5. The VULCAN Petawatt facility allows experimental access to regimes where $a_0 \gg 1$ (and in the experiment reported here $a_0 \approx 15$).

During this experiment the laser consistently produced 650 fs duration pulses delivering $\sim$180 J on target. These pulses were focused with an $f/3$ off-axis parabolic mirror to produce a focal spot with an intensity FWHM (full width half maximum) of ~10 μm, thus generating intensities greater than 3×10^{20} W cm^{-2}.

The experimental setup is shown in Fig. 4. The gas jet used has a 2 mm diameter supersonic nozzle and could produce plasma electron densities between 5×10^{18} and 2×10^{20} cm^{-3}. The density was controlled by varying the backing pressure behind the value of the gas jet. The density was measured using the forward Raman scattering signal. Two series of shots were performed in this particular experiment, one with helium and the other with deuterium. Since He^{2+} and D^+ have the same charge to mass ratio there should

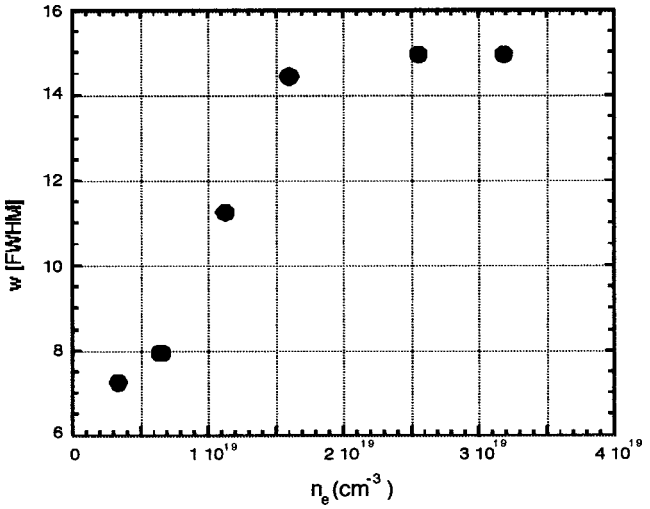

FIG. 3. Electron beam divergence measurements for 50 TW laser interactions at varying plasma densities. The measurement was performed using γ activation of an array of copper pieces.

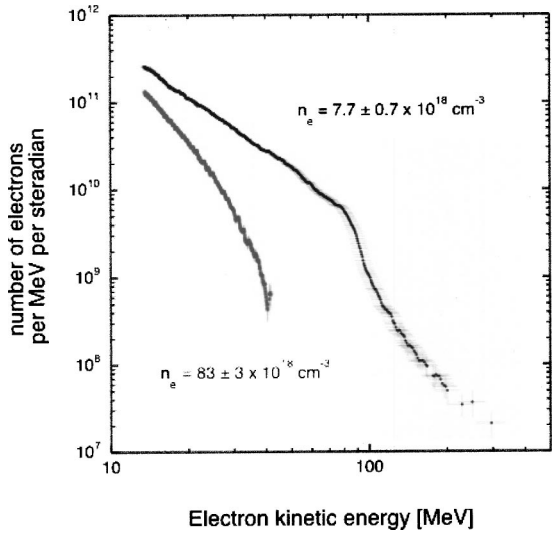

FIG. 5. Electron energy spectra at two densities from Petawatt interactions. The highest energy electrons are observed at an electron density of $n=(7.7\pm0.7)\times10^{18}$ cm^{-3}. At this density the spectrum is non-Maxwellian. For densities higher or lower than this the spectra are broadly similar and can be better described by an effective temperature.

be little qualitative difference in the two data sets (which indeed was observed to be the case).

The electrons accelerated along the axis of laser propagation were measured using a high field magnetic spectrometer. The electrons exit the highly shielded main vacuum chamber through a small (25 mm) diameter tube to a secondary vacuum vessel—and this helps to reduce the level of background signal from low energy x rays and scattered electrons. The entrance to the spectrometer is a 5 mm diameter hole that serves to collimate the electron beam to ensure sufficient energy resolution. The specially designed vacuum chamber allows the electron beam to pass between the pole pieces of an electromagnet that deflects the electrons off-axis. The correspondence between electron energy and deflection from the axis is determined by using a charged particle tracking code.

In these experiments, electrons are detected using an image plate (Fuji BAS1800II) which is a reusable film sensitive to ionizing radiation.[17] Two sections of an image plate are used, one to measure the electron signal, below axis, and another to measure the background signal above the axis. Since the background is due to x rays from the interaction itself or from bremsstrahlung radiation emitted by the electrons as they pass through material before the detector plane it is assumed that the background is symmetric above and below the axis.

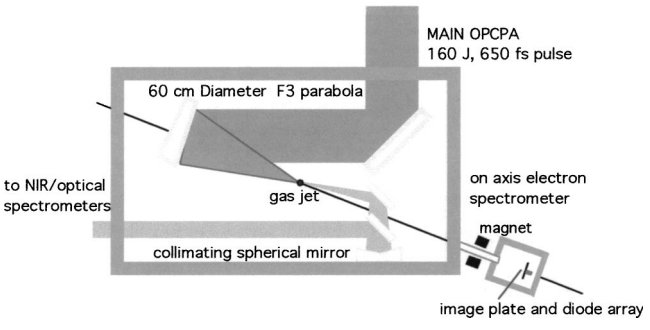

FIG. 4. Schematic of experimental setup for Petawatt electron acceleration experiments.

The relationship between image plate signal intensity and energy deposited in the plate is close to linear. This has been confirmed by previous studies.[17] The direct relationship between the number of electrons and the signal was calculated by placing a diode array directly behind the image plates. The ion implanted diodes used have an absolutely calibrated response to the number of electrons incident and by calculating the energy lost by the electrons as they travel through the plate before reaching the diodes it is possible to cross calibrate the diode and image plate signals.

The image plate data exhibits a much larger dynamic range than the diodes and the image nature of the data allows much better noise discrimination. The resolution of the image plates, although not as high as x-ray film, is significantly better than the diode array. The combination of the resolution and size of the image plates (each is 250 mm long) allows a reasonably broad energy range (for example, 10–250 MeV) to be measured in a single shot.

The laser-plasma interaction was also diagnosed by measuring the transmitted spectrum of the laser. A portion of the transmitted beam was collimated and transported out of the vacuum chamber to a pair of near-infrared spectrometers; charge-coupled device (CCD) cameras recorded the spectra on each shot at two different dispersions.

Figure 5 shows a number of electron energy spectra obtained from shots with helium gas. These shots have been selected to show the trend observed as the density of the gas jet was varied. Electrons were accelerated to relativistic energies at all densities. At low densities ($n_e<10^{19}$ cm^{-3}) the electron energy spectrum could be characterized by an effective temperature, that is, the number of electrons N with energy E was given by $N(E)\propto\exp(-E/T_{\text{eff}})$. As the density was increased the maximum energy observed increased,

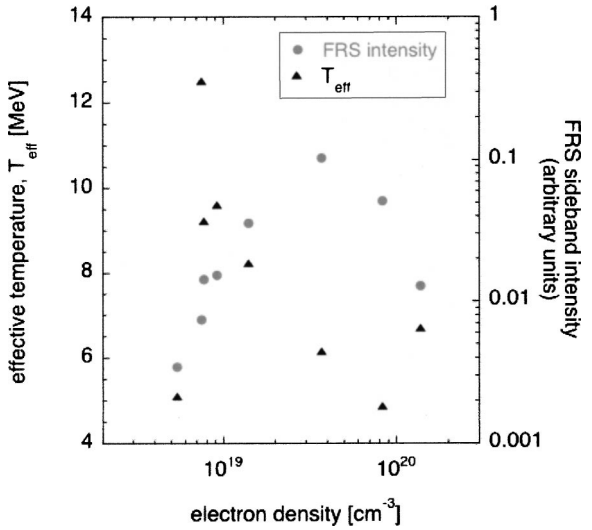

FIG. 6. Variation of observed electron "temperature" and amount of forward Raman scattered (FRS) light with plasma density in helium gas jet. Note the lack of correlation of FRS and acceleration.

along with T_{eff}. The spectrum also begins to take on a non-Maxwellian form. At $n_e=(0.7\pm0.1)\times10^{19}$ cm^{-3} the acceleration is significantly enhanced, and the energy observed was up to about 300 MeV. The maximum is, in this case, limited by the noise level on the image plate. As the density was increased above 10^{19} cm^{-3} the acceleration was observed to be less effective and the spectrum regains its effective temperature form.

Figure 6 shows explicitly how the acceleration varied with electron density for helium shots. This energy varies strongly with density exhibiting an apparent peak around 1×10^{19} cm^{-3}. The shots taken with deuterium gas produced similar spectra and show the same variation with density, although the optimum density is shifted slightly to $(1.4\pm0.2)\times10^{19}$ cm^{-3}.

Figure 6 also shows the relationship between the amount of forward Raman scattering (FRS) observed and the electron density. It is clear that the production of high energy electrons and FRS are uncorrelated. This is in marked difference to previous experiments,[5,13] and indicates that the acceleration mechanism cannot be SM-LWFA as in the experiments described in Sec. II.

A study by Gahn *et al.*[18] with 200 fs, 0.25 J pulses showed an enhanced acceleration at 2×10^{20} cm^{-3}. In that experiment there was strong evidence that electron acceleration is strongly correlated with channel formation and magnetic field generation. Simulations[19] indicated that when the betatron motion of the electron in the self-generated magnetic field is resonant with the relativistic motion of the particle in the laser field, electrons can pick up energy directly from the laser pulse [direct laser acceleration (DLA)]. This is similar to an inverse free-electron laser mechanism and can occur efficiently when the laser power becomes significantly greater than the critical power for self-focusing.

However the divergence of the beam suggested from these previous lower intensity experiments and simulations is large. With the much smaller divergence observed in the

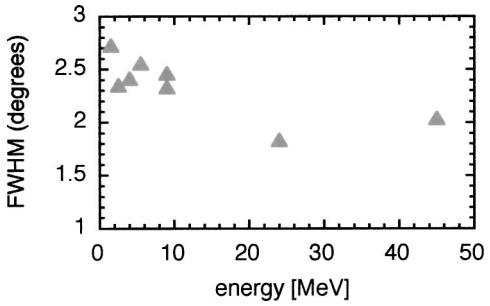

FIG. 7. Beam divergence measurements for a shot at different electron energies taken with activation of a stack of copper plates (note that the divergence is significantly less than in 50 TW experiments, Fig. 3).

VULCAN Petawatt experiments (see Fig. 7) the mechanism of direct laser acceleration seems to be more complex and may involve stochastic "dephasing" processes[20,21] and the combined effect of the laser electric field with the electrostatic field due to charge displacement during the intense laser plasma interaction.

A number of 2D-3V (2 spatial, 3 velocity dimension) particle in cell (PIC) code simulations using the code OSIRIS (Ref. 22) (developed by UCLA) have been performed on a 24 node BEOWULF cluster at Imperial College showing that a form of direct acceleration by the laser is the dominant acceleration mechanism in the results reported here. The PIC code simulations show the bunching of the accelerated electrons at twice the laser frequency and also that the electrons are accelerated within the laser pulse, the maximum energy coinciding with the maximum laser intensity.

The PIC code simulations have also indicated a possible cause of the observed density-acceleration dependence. Simulations were performed at various densities simulating realistic laser pulses incident on a fully ionized plasma having a linear density ramp from vacuum up to bulk plasma density over ~600 μm (this is consistent with the type of nozzle used in these experiments). Each simulation was run for passage throughout the gas jet target. Figure 8 shows images of the laser intensity after 2.6 ps in two simulations, the first is at low density (1×10^{19} cm^{-3}) and the second is at higher density (1.4×10^{20} cm^{-3}). In the high density run the laser undergoes strong self-focusing and filamentation.[23] The filamented laser then undergoes a hosing type instability. This filamentation and hosing has not occurred in the low density case.

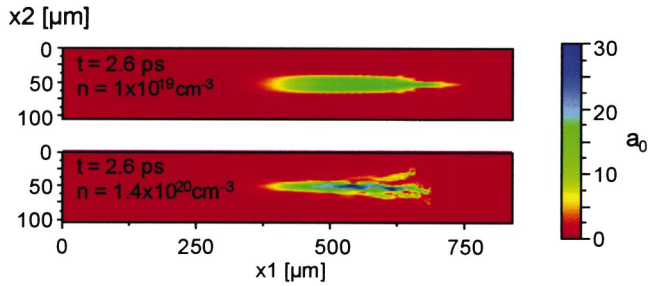

FIG. 8. (Color). Laser energy distribution of Petawatt laser pulses after 2.6 ps of propagation using the OSIRIS PIC code. Note that at higher plasma density the laser pulse is very filamented.

If this hosing instability occurred at high densities in the experiment, it may be responsible for reducing the effective intensity during the interaction as well as perhaps moving the electron beam off axis, such that the highest energy electron did not enter the electron spectrometer (in simulations the electron beam closely follows the laser pulse).

IV. MONOENERGETIC BEAM PRODUCTION USING ULTRASHORT PULSES

We have also performed electron acceleration experiments using a third laser system, the high power ultrashort pulse titanium:sapphire ASTRA laser system at the Central Laser Facility of the Rutherford Appleton Laboratory. The laser pulses ($\lambda = 800$ nm, $E = 450$ mJ, $t = 40$ fs) were focused with an $f/16.7$ off axis parabolic mirror onto the edge of a 2 mm long supersonic jet of helium gas to produce intensities on the order of 1.3×10^{18} W cm^{-2}. The electron density n_e as a function of backing pressure on the gas jet was determined by measuring the frequency shift ($\Delta\omega = \omega_{pe}$, where ω_{pe} is the electron plasma frequency) of satellite wavelengths generated by forward Raman scattering in the transmitted light. The plasma density was again observed to vary linearly with backing pressure within the range $n_e = 3 \times 10^{18}$ cm^{-3}–5×10^{19} cm^{-3}. In this density range the wavelength of relativistic plasma waves produced (i.e., $\lambda_p = 2\pi\omega_{pe}/c$) is between 1 and 10 times the laser pulse length $c\tau_L$. For laser pulses which are less than the plasma wavelength, relativistic plasma waves can be generated "resonantly" in the wake of the pulse—while in the regime in which the laser pulse length is longer than the plasma wavelength, high intensity interactions are required to drive an instability in which the plasma waves are produced via "self-modulation" of the laser pulse envelope at the plasma frequency. In the work described here it is likely that self-modulation is initially the dominant mechanism for plasma wave generation. In our experiments the plasma waves are driven so that they grow until wave breaking occurs. This is a phenomenon which takes place at very large amplitudes such that the wave motion becomes so nonlinear that wave energy is transferred directly into particle energy and the plasma wave loses coherence. Electrons which reach relativistic energies from wave breaking of a plasma wave can be "injected" into an adjacent plasma wave where they can pick up even more energy (the "cold" wave breaking electric-field amplitude for electron plasma waves is given by $E = m_e c\omega_{pe}/e$). Note that in a regime between SM-LWFA and LWFA lies the F-LWFA (*forced* laser wakefield accelerator) where a short pulse is used which is only slightly longer than the resonant pulse length. This pulse is consequently focused and compressed by the wave to produce large amplitude plasma waves which can break.

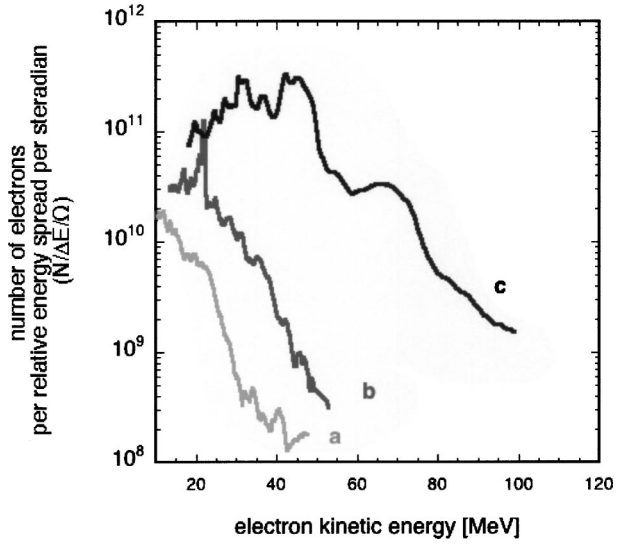

FIG. 9. Measured electron spectra from interaction of ASTRA laser at various densities (a) $n_e = 5 \times 10^{19}$ cm^{-3}, (b) $n_e = 3 \times 10^{19}$ cm^{-3}, (c) $n_e = 1.6 \times 10^{19}$ cm^{-3} at $E = 350$ mJ, $t = 40$ fs.

Note that in the experiment described here the electron energy spectrum was measured using an on-axis magnetic spectrometer similar to that in the Petawatt experiments. The electrons were also simultaneously measured with the high resolution image plate detectors as well as using a much lower resolution array of diodes. The spectrometer magnet, image plates, and diodes were set up to measure the spectrum over a wide energy range in a single shot.

Other diagnostics used in this case included the simultaneous measurement of the transmitted laser spectrum and transverse optical probing of the interaction with a frequency doubled laser probe beam. This was used to produce images of the plasma via shadowgraphy, and was independently timed so it could also be used to measure prepulse effects and plasma channel formation.

Electron acceleration was observed over a range of electron densities. With the plasma density below 7.3×10^{18} cm^{-3} no energetic electrons were observed (this corresponds to $c\tau_L < 2.5\lambda_p$). In this regime the growth rate of the self-modulation instability is too low for a plasma wave to reach wave-breaking amplitudes.

As the density was increased above 7×10^{18} cm^{-3}, very high energy electrons were suddenly produced with the most energetic electrons reaching up to 100 MeV. The output beam divergence was also measured and was found to be less than 5°. However the most interesting aspect of these spectra is that, in this regime, the electron energies were exceptionally non-Maxwellian and, indeed, generally consisted of one or more narrow spiky features—each of which could have an energy bandwidth of less than 20% (see Fig. 9). This is in contrast to the energy spectra of previous laser acceleration experiments in which 100% energy spreads are observed. As the density was increased in our experiments, the peak energy of the observed electrons was observed to decrease and the spectra begin to assume a broad Maxwellian shape which was characteristic of previous experiments in the SM-LWFA regime.

The likely explanation for the difference observed in these spectra is due to the timing of the "injection" of electrons into the relativistic plasma wave. It appears that as the plasma wave reaches an amplitude which is just sufficient for wave breaking only a few electrons are able to "fall" into the accelerating portion of the adjacent waves in the wake, and so all of these electrons see an almost identical acceleration gradient. Since successive waves in the wakefield are of dif-

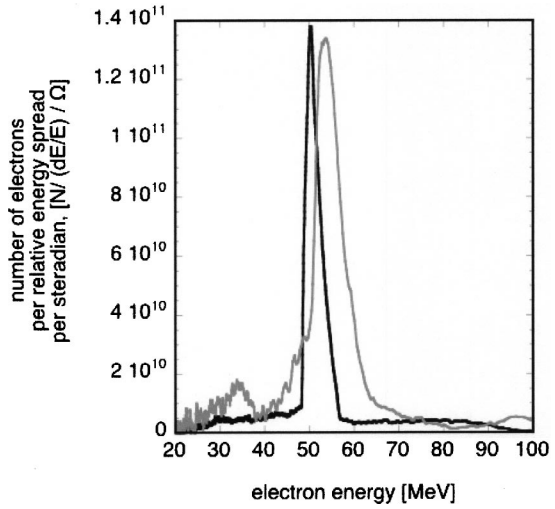

FIG. 10. Two measured electron spectrum with $E=500$ mJ laser at a density of 2×10^{19} cm^{-3}. Shots are taken from the same shot series.

ferent amplitude (i.e., they have differing accelerating gradients) successive trapped bunches will be accelerated to different energies.

In addition, because of the low density these electron bunches are not dephased since the propagation distance is only about 1 mm (or the length of the gas jet plasma). The dephasing distance is the length over which an electron outruns the plasma wave, and begins to be deaccelerated by the wave, and is given as $L_d=2\pi c\omega^2/\omega_{pe}^3$. For our experiments the conditions which showed the clearest, most reproducible evidence of these electron beams were those in which the dephasing length, the gas jet length, and the confocal parameter of the laser beam are all roughly 1 mm.

In contrast at higher densities the dephasing distance is much shorter than the interaction distance and so a "randomized" or quasi-Maxwellian distribution of electrons would emerge from the plasma.

In the final set of experiments the energy of the laser pulse was increased to about 500 mJ. These experiments showed that for the densities used to obtain "bumpy" spectra in the lower energy situations that very monoenergetic spectra could be observed. This is shown in Fig. 10 in which two electron spectra are shown—from the same series of shots. The spectra can be reasonably reproducible and the narrowest spectrum shows a beam at 52 MeV with an energy spread $(\Delta E/E)$ of less than 5%. The beam divergence in this regime is also extremely low (see Fig. 11).

This phenomenon is indeed what is observed when two-dimensional particle-in-cell simulations of the interaction were performed using the code OSIRIS and it was found that for relatively low plasma densities as the plasma waves grow to an amplitude such that it they are observed to break—a group of electrons is injected into a particular phase position into the plasma wave and this group of electrons can be accelerated relatively uniformly (Fig. 12).

When the pulse is fully self-focused, some relativistic electrons have appeared, but at quite low energies. This is where wave breaking occurs. As the laser pulse front begins to steepen, the wakefield amplitude grows and the electron energies increase until the pulse reaches its maximum peak intensity. At this point the electron energies are clearly "bunched" at a particular energy. After this time the average electron energies begin to drop and the distribution of electron energies is randomized—since the propagation distance is beyond the dephasing length for this interaction.

The diminishing energies are also caused by the "erosion" of the pulse leading edge, coupled with the nonlinear lengthening of the plasma wavelength in the wake which slows the electrons. This process continues so that the bunch again enters a region of accelerating field and the energies increase once more. When the wake reaches its highest amplitude the trapped electrons are completely dephased with respect to the plasma wave.

It is clear from simulations that in our experiments the "bunches" of electrons are produced due to wave breaking in the immediate vicinity of the laser pulse. These electrons are then accelerated through the entire length of the plasma—which is shorter than the dephasing distance. Consequently, the bunch of electrons can remain relatively monoenergetic after leaving the plasma. The requirements for this regime

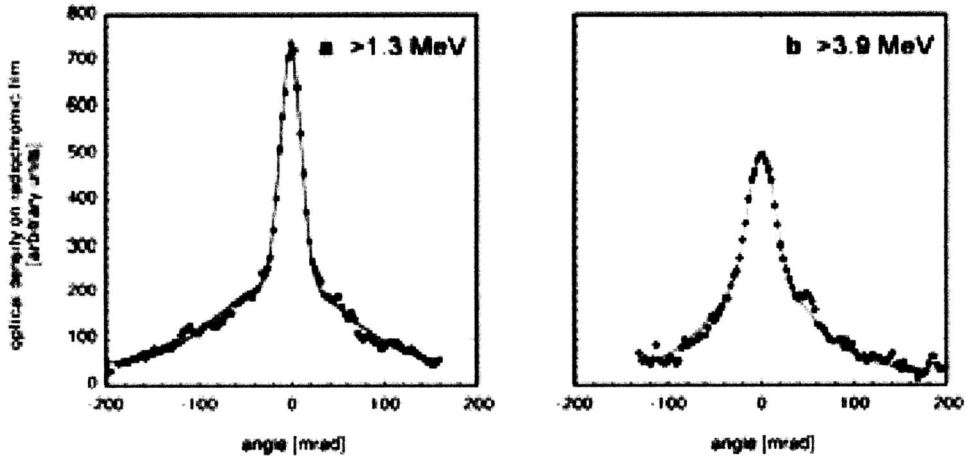

FIG. 11. Beam divergence measurements for ASTRA experiments measured using radiochromic film (a) gives beam profile above 1 MeV and (b) gives the beam profile above 4 MeV. These are similar and less than 2°.

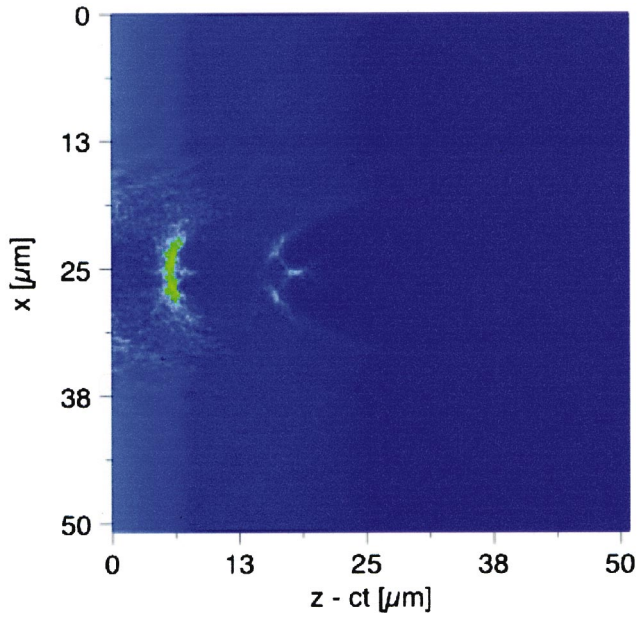

FIG. 12. (Color). Two dimensional OSIRIS simulation of ASTRA interaction (the electron density is shown during wave breaking). The injected electron bunch resulting from wave breaking of the plasma wave are clearly shown as the laser pulse propagates into vacuum (from left to right).

are that the plasma density has to be high enough so that wave breaking is easily achieved, but low enough so that the electron bunches produced are not dephased before they leave the plasma.

To summarize, we have demonstrated that the ASTRA laser can be used to produce relativistic bunches of electrons with energies approaching 100 MeV. Accelerated electrons are not observed below a minimum density, but at densities slightly higher than this monoenergetic electron beams can be clearly observed in the spectrum. As the plasma density is increased such structures are randomized still further by the dephasing of the accelerated electrons with the plasma waves and the energy spread of 100% is observed.

The observation that laser produced plasmas alone can produce monoenergetic electron beams suggests that such sources hold great promise for future development of table-top particle accelerators and that a wide range of applications may soon become possible.

V. CONCLUSIONS

In summary, the experiments on the VULCAN Petawatt facility has successfully accelerated electrons up a maximum energy up to about 300 MeV with low divergence. This is the highest energy observed from any laser-plasma interaction to date. It appears that the increase in intensity has moved VULCAN from operating in the SM-LWFA regime to one where a form of DLA is dominant.

On the other hand a reduction in the pulse length (and increase in the focal length) has shown that the SM-LWFA moves into a completely different regime in which relativistic monoenergetic electron beams can be produced. This seems to be the most attractive route for further scientific exploration as well as for the development of applications.

ACKNOWLEDGMENTS

The authors acknowledge the assistance of the staff of the Central Laser Facility of the Rutherford Appleton Laboratory in the execution of this work as well as the support of the UK Engineering and Physical Sciences Research Council (EPSRC). They gratefully acknowledge the OSIRIS consortium which consists of UCLA/IST(Portugal)/USC for the use of OSIRIS.

[1] M. D. Perry and G. Mourou, Science **264**, 917 (1994).
[2] M. H. Key, M. D. Cable, T. E. Cowan *et al.*, Phys. Plasmas **5**, 1966 (1998).
[3] M. Tatarakis, I. Watts, F. N. Beg, E. L. Clark, A. E. Dangor, M. G. Haines, P. A. Norreys, M. Zepf, and K. Krushelnick, Nature (London) **415**, 280 (2002).
[4] C. Joshi and T. Katsouleas, Phys. Today **56**(6), 47 (2003); P. Sprangle, E. Esarey, A. Ting, and G. Joyce, Appl. Phys. Lett. **53**, 2146 (1988); K. Nakajima, D. Fisher, T. Kawakubo *et al.*, Phys. Rev. Lett. **74**, 4428 (1995); D. Umstadter, S. Y. Chen, A. Maksimchuk, G. Mourou, R. Wagner *et al.*, Science **273**, 472 (1996); A. Ting, C. I. Moore, K. Krushelnick, C. Manka, E. Esarey, P. Sprangle, R. Hubbard, H. R. Burris, R. Fischer, and M. Baine, Phys. Plasmas **4**, 1889 (1997).
[5] M. I. K. Santala, Z. Najmudin, K. Krushelnick, E. L. Clark, A. E. Dangor, V. Malka, J. Faure, R. Allott, and R. J. Clarke, Phys. Rev. Lett. **86**, 1227 (2001).
[6] E. L. Clark, K. Krushelnick, M. Zepf, F. N. Beg, A. Machacek, P. A. Norreys, M. I. K. Santala, M. Tatarakis, I. Watts, and A. E. Dangor, Phys. Rev. Lett. **85**, 1654 (2000); K. Krushelnick, E. L. Clark, Z. Najmudin *et al.*, *ibid.* **83**, 737 (1999).
[7] R. D. Edwards, M. A. Sinclair, T. J. Goldsack *et al.*, Appl. Phys. Lett. **80**, 2129 (2002).
[8] T. Tajima and J. M. Dawson, Phys. Rev. Lett. **43**, 267 (1979).
[9] S. P. D. Mangles, C. D. Murphy, Z. Najmudin *et al.*, Nature (London) **431**, 535 (2004).
[10] J. Faure, Y. Glinec, A. Pukhov *et al.*, Nature (London) **431**, 541 (2004); C. G. R. Geddes, C. Toth, J. van Tilborg *et al.*, *ibid.* **431**, 538 (2004).
[11] S. Tochitsky, R. Narang, C. V. Filip *et al.*, Phys. Rev. Lett. **92**, 095004 (2004).
[12] B. Walton, Z. Najmudin, M. S. Wei *et al.*, Opt. Lett. **27**, 2203 (2002).
[13] A. Modena, Z. Najmudin, A. E. Dangor, C. E. Clayton, K. A. Marsh, C. Joshi, V. Malka, C. B. Darrow, C. Danson, D. Neely, and F. N. Walsh, Nature (London) **377**, 606 (1995).
[14] V. Malka, S. Fritzler, E. Lefebvre, M.-M. Aleonard, F. Burgy, J.-P. Chambaret, J.-F. Chemin, K. Krushelnick, G. Malka, S. P. D. Mangles, Z. Najmudin, M. Pittman, J.-P. Rousseau, J.-N. Scheurer, B. Walton, and A. E. Dangor, Science **298**, 1596 (2002).
[15] F. Amiranoff, S. Baton, D. Bernard *et al.*, Phys. Rev. Lett. **81**, 995 (1998).
[16] Z. Najmudin, R. Allott, F. Amiranoff *et al.*, IEEE Trans. Plasma Sci. **28**, 1084 (2000).
[17] S. G. Gales and C. D. Bentley, Rev. Sci. Instrum. **75**, 4001 (2004); K. Tanaka, *ibid.* **76**, 013507 (2005).
[18] C. Gahn, G. D. Tsakiris, A. Pukhov, J. Meyer-ter-Vehn, G. Pretzler, P. Thirolf, D. Habs, and K. J. Witte, Phys. Rev. Lett. **83**, 4772 (1999).
[19] A. Pukhov, Rep. Prog. Phys. **66**, 47 (2003); A. Pukhov, Z. M. Sheng, and J. Meyer-ter-Vehn, Phys. Plasmas **6**, 2847 (1999).
[20] J. Meyer-ter-Vehn and Z. M. Sheng, Phys. Plasmas **6**, 641 (1999).
[21] S. P. D. Mangles, B. R. Walton, Z. Najmudin *et al.* (unpublished).
[22] R. Hemker, Ph.D. thesis, UCLA, 2000.
[23] Z. Najmudin, K. Krushelnick, M. Tatarakis *et al.*, Phys. Plasmas **10**, 438 (2003).